Optimal trajectory and tracking control system for a helicopter safe landing in autorotation

Giulio Avanzini, giulio.avanzini@unisalento.it, University of Salento (Italy)

Emanuele L. de Angelis, emanuele.deangelis4@unibo.it, University of Bologna (Italy)

Guido De Matteis, guido.dematteis@uniroma1,it, Sapienza Università di Roma (Italy)

Daniele Fattizzo, daniele.fattizzo2@unibo.it, University of Bologna (Italy)

Fabrizio Giulietti, fabrizio.giulietti@unibo.it, University of Bologna (Italy)

Alessandro Zavoli, alessandro.zavoli@uniroma1,it, Sapienza Università di Roma (Italy)

Abstract

In case of engine failure autorotation represent a safe maneuver for helicopter emergency landing. In autorotation, the rotor is no longer engine-powered but keeps rotating thanks to the impinging flow. During the descent, rotor angular velocity is constant for a given setting of collective pitch and the power dissipated by its rotation is compensated by a loss of potential energy during the descent. A steady descent is then possible down to a fixed altitude where, exploiting rotor residual energy, it is possible to perform a flare bringing the helicopter to minimum touch down velocity.

For small scale helicopters an autonomous control system for autorotation can reduce damages and economic losses, saving the rotorcraft and its payload in case of an engine failure.

In this paper, a preliminary investigation on steady descent conditions in autorotation, and the design of a possible flare maneuver has been made through a model-based design approach. Also, a closed loop control system has been developed, to perform the two main phases of autorotation maneuver. Simulations results show the suitability of the proposed approach for a wide range of initial conditions (altitude and advancing velocity).

NOMENCLATURE

a_0	Rotor coning angle (rad)
a_1	Longitudinal rotor tip path plane deflection angle in rotor-hub system (rad)
A_{1c}	Lateral cyclic pitch measured from hub plane in Wind-Hub axes system(rad)
A_{1s}	Lateral cyclic pitch measured from hub plane in Hub-Body axes system(rad)
b_1	Lateral rotor tip path plane deflection angle in rotor-hub system (rad)
B_{1c}	Longitudinal cyclic pitch measured from hub plane in Wind-Hub axes system(rad)
B_{1s}	Longitudinal cyclic pitch measured from hub plane in Hub-Body axes system(rad)
$\widetilde{D}$	Damping matrix for flapping
e	Flapping hinge offset (m)
$\tilde{f}$	Forcing function for flapping
$\widetilde{K}$	Stiffness matrix for flapping
K_1	Pitch-flap coupling ratio
M_β	Blade weight moment about the flapping hinge (N·m)
M_{tot}	Total mass (kg)
U_T	Blade element velocity on the hub plane (m/s)
U_P	Blade element velocity normal to the hub plane (m/s)

Presented at 47th European Rotorcraft Forum, United Kingdom, 7-9th September, 2021

$\mathbf{I} = \begin{bmatrix} I_{xx} & I_{xy} & I_{xz} \\ I_{yx} & I_{yy} & I_{yz} \\ I_{zx} & I_{zy} & I_{zz} \end{bmatrix}$	Inertia tensor (kg/m^2)
$\mathbf{F}_{(\cdot)} = [X \quad Y \quad Z]^T$	Forces vector (N)
$\boldsymbol{M}_{(\cdot)} = [L \quad M \quad N]^T$	Moments vector (Nm)
$\mathbf{V}_{(\cdot)} = [u \quad v \quad w]^T$	Linear velocity vector (m/s)
$\boldsymbol{\omega}_{(\cdot)} = [p \quad q \quad r]^T$	Angular velocity vector (rad/s)
β	Blade flapping (rad)
ε	Hinge offset ratio
μ	Advance ratio
λ	Inflow ratio
ϕ, θ, ψ	Roll, pitch, yaw Euler angles (rad)
θ_0	Blade root collective pitch (rad)
Ω	Rotor angular velocity (rad/s)
	Subscripts
b	Body frame
cl	Clockwise
ccl	Counter-clockwise
E	Earth fixed NED frame
e	Equilibrium condition
fus	Fuselage
h	Hub-Body frame
LV	Local-Vertical frame
mr	Main rotor
sd	Steady descent
w	Wind-Hub frame
	Superscripts
a	Aerodynamic
e	External
g	Gravitational

1. INTRODUCTION

Engine failure represents one of the most critical situations for any aircraft. This situation becomes possibly dramatic for single-engine rotorcraft, provided that in the case of total power loss, a safe landing maneuver in autorotation needs to be performed. For manned helicopters, the ability of the pilot is of primary importance for the success of the maneuver and therefore for the safety of the pilot himself. Moreover a good landing avoids or minimizes damage to the aircraft reducing economic losses. For an unmanned aerial vehicle the possibility of an emergency landing maneuver is often neglected and shot-down systems are usually implemented to allow the pilot to interrupt the flight when the aircraft is out control or out of a nominal condition such as an engine failure, after a safe zone has been reached. Danger for people in this case is much reduced and the economic loss can be sometimes negligible. However there are conditions where costs and risks increases, especially in the case of important payloads which should be saved. For fixed wing aircrafts this problem can be managed considering a parachute for the payload. In the case of helicopters, the choice of a safe parachute presents several difficulties. That's why an autonomous control system able to perform an autorotation maneuver becomes in this case a good solution.

In autorotation the main task is to reduce sink rate to minimum value minimizing the impact velocity and therefore damages. The optimal trajectory to minimize touch down velocity has been evaluated in [1] considering a very simple model of the vertical dynamics of the helicopter. Similar optimal approach, but with a more complex cost function and dynamics model have been considered in [2] and in [3] where, in the latter, an optimal trajectory and control system for the tracking have been evaluated.

Scope of this paper is to give a preliminary analysis on the autorotation, considering a complete dynamic model of a small scale helicopter and evaluating different flight conditions for a steady descent in autorotation and then for the flare. A suitable autorotation maneuver has been designed, and a control system has been developed to simulate it in closed loop.

2. MATHEMATICAL MODELLING

2.1. Aircraft dynamics

An overview of main equations and assumptions for the dynamic model of the Helicopter is here given.

2.1.1. Reference frames and coordinate transformation

Six orthogonal reference frames are introduced: Hub-Wind; Hub-Body, Body, Aircraft and Local Wind. In particular, the term "Hub" means that the origin of the coordinate system is at the main rotor hub centre.

The terms "Wind" and "Body" indicate where the three axes point.

1. An Earth-fixed North–East-Down frame, $\mathbb{F}_E = \{O;\ \boldsymbol{x}_E, \boldsymbol{y}_E, \boldsymbol{z}_E\}$. This frame is inertial under the assumption of flat and non-rotating Earth.
2. Hub Wind Frame $\mathbb{F}_{hw} = \{H;\ \boldsymbol{x}_{hw}, \boldsymbol{y}_{hw}, \boldsymbol{z}_{hw}\}$. This frame is used in calculation of rotor forces and moments. Its origin is the rotor hub. $\mathbf{z}_{hw}$ axis is aligned with the rotor shaft, pointing upward. $\mathbf{x}_{hw}$ axis (horizontal) is aligned with the component of relative wind normal to the shaft axis. $\mathbf{y}_{hw}$ axis completes the right-handed orthogonal set.
3. Hub Body Frame $\mathbb{F}_{hb} = \{H;\ \boldsymbol{x}_{hb}, \boldsymbol{y}_{hb}, \boldsymbol{z}_{hb}\}$. $\mathbf{z}_{hb}$ axis is aligned with rotor shaft, pointing upward. This system coincides with the hub-wind system when the sideslip β_w is zero.
4. Body Fixed Frame $\mathbb{F}_b = \{P;\ \boldsymbol{x}_b, \boldsymbol{y}_b, \boldsymbol{z}_b\}$. Origin is located at the centre of gravity of the rotorcraft. $\mathbf{x}_b$ axis points in forward direction, it's aligned with the longitudinal axis of the vehicle; $\mathbf{z}_b$ is perpendicular to $\mathbf{x}_b$ in the longitudinal plane pointing downward, and $\mathbf{y}_b$ axis completes the right-hand system. All forces and moments used in the body equations of motion are expressed relative to this system.
5. Wind Frame $\mathbb{F}_w = \{R;\ \boldsymbol{x}_w, \boldsymbol{y}_w, \boldsymbol{z}_w\}$. These axes are used to calculate lift and drag forces on the fuselage. The origin is in the fuselage pressure centre.
6. Local Vertical Frame $\mathbb{F}_{LV} = \{P;\ \boldsymbol{x}_{LV}, \boldsymbol{y}_{LV}, \boldsymbol{z}_{LV}\}$. Origin is at the centre of gravity and axes are parallel to the inertial frame.

Rotor flapping dynamics assessment and rotor forces and moments calculation require linear and angular velocity vectors and acceleration vector as expressed in the Hub-Body system and the angle of sideslip at the hub. The cyclic pitch is also requested in Hub-Wind system.
In this respect, the velocity vector at the hub is written as follows:

(1) $$\boldsymbol{V_h} = \boldsymbol{\Pi_{hb}}[\boldsymbol{V_b} + \boldsymbol{\omega_b} \times \boldsymbol{r_b}]$$

whereas angular velocity and acceleration are given by:

(2) $$\boldsymbol{\omega_h} = \boldsymbol{\Pi_{hb}}\boldsymbol{\omega_b}$$

(3) $$\dot{\boldsymbol{\omega}}_{\boldsymbol{h}} = \boldsymbol{\Pi_{hb}}\dot{\boldsymbol{\omega}}_{\boldsymbol{b}}$$

where $\boldsymbol{\Pi_{hb}}$ is the rotational matrix from Body to Hub-Body system. Since rotor shafts is tilted in XZ plane with an angle i_s, Π_{hb} is written as:

(4) $$\boldsymbol{\Pi_{hb}} = \begin{bmatrix} \cos i_s & 0 & \sin i_s \\ 0 & 1 & 0 \\ -\sin i_s & 0 & \cos i_s \end{bmatrix}$$

Calculated Wind-Hub system components are then rotated to be implemented into the 6-DOF equations of motion:

(5) $$\begin{bmatrix}(\cdot)_x \\ (\cdot)_y\end{bmatrix}_{wh} = \begin{bmatrix}\cos\beta_w & \sin\beta_w \\ -\sin\beta_w & \cos\beta\_w\end{bmatrix}\begin{bmatrix}(\cdot)_x \\ (\cdot)_y\end{bmatrix}_{hb}$$

Where

(6) $$\beta_w = \sin^{-1}\frac{v_h}{\sqrt{v_h^2+u_h^2}}$$

is the sideslip angle.

2.1.2. Dynamic model

Helicopter dynamics model considers the following state vector:

(7) $$\boldsymbol{x} = [\boldsymbol{V_b}; \boldsymbol{\omega_b}; \boldsymbol{a}; \lambda_i; \Omega]$$

and command vector:

(8) $$\boldsymbol{u} = [\theta_0; A_{1s}; B_{1s}; \theta_{tr}]$$

Where $\boldsymbol{V_b} = [u\ v\ w]'$ and $\boldsymbol{\omega_b} = [\mathrm{p\ q\ r}]'$ are the rigid body 6dofs in the body reference frame, $\boldsymbol{a} = [a_0\ a_1\ b_1]'$ is the vector of flapping angles, $\lambda_i = \frac{V_i}{\Omega R}$ is the inflow ratio due to rotor thrust induced velocity, and Ω is the main rotor angular speed. The command vector components are: the collective pitch θ_0, the lateral and longitudinal pitch angle in the Hub-body frame A_{1s}, B_{1s}, and the tail rotor pitch θ_{tr}.

The equations involved are:

- Equations of motions in body reference frame

(9) $$\begin{cases} \dot{\boldsymbol{V}}_{\boldsymbol{b}} = -\boldsymbol{\omega_b} \times \boldsymbol{V_b} + \boldsymbol{F_b}/M_{tot} \\ \dot{\boldsymbol{\omega}}_{\boldsymbol{b}} = \boldsymbol{I}^{-1}[-\boldsymbol{\omega_b} \times (\boldsymbol{I}\boldsymbol{\omega_b}) + \boldsymbol{M_b}] \end{cases}$$

Where forces and moments are the sum of aerodynamic and gravitational effects for all the helicopter subsystems (main rotor, tail rotor, fuselage).

(10) $$\begin{cases} \boldsymbol{F_b} = \boldsymbol{F_{mr}^a} + \boldsymbol{F_{tr}^a} + \boldsymbol{F_{fus}^a} + \boldsymbol{W} \\ \boldsymbol{M_b} = \boldsymbol{M_{mr}^a} + \boldsymbol{M_{tr}^a} + \boldsymbol{M_{fus}^a} \end{cases}$$

- Flapping dynamics equation

(11) $$\ddot{\boldsymbol{a}} = -\widetilde{\boldsymbol{D}}\dot{\boldsymbol{a}} - \widetilde{\boldsymbol{K}}\boldsymbol{a} + \tilde{\boldsymbol{f}}$$

Where the components of the flapping vector $\boldsymbol{a}$ represent the time variant coefficients of the tip path-plane flapping equation:

(12) $$\beta(t,\psi) = a_0(t) + a_1(t)\cdot\cos\psi + b_1(t)\cdot\sin\psi$$

With $\beta(\psi,t)$ flapping angle of the blade having an azimuth angle ψ. The flapping model is derived in [4].

- Inflow dynamics equation

(13) $$\dot{\lambda}_i = \frac{3\pi}{4}\left\{\frac{C_t}{2} - \lambda_i\sqrt{\mu^2+\lambda^2}\right\}$$

Where C_t is the main rotor thrust coefficient, $\mu = \frac{\sqrt{u_h^2+v_h^2}}{\Omega R}$ is the advance ratio with respect to hub-body frame and $\lambda = \frac{w_h}{\Omega R} - \lambda_i$ is the total inflow ratio.

Here a uniform dynamic model, derived from [5], has been chosen to simplify analytical evaluation of the main rotor forces and moments.

- Rotor dynamics equation

Calling I_{mr} and I_{tr} the rotational inertia moments of the main and tail rotor, and τ the transmission ratio between main and tail rotor rotational speeds, the kinetic energy of the rotors is:

$$T_{rotors} = \frac{1}{2}I_{mr}\Omega_{mr}^2 + \frac{1}{2}I_{tr}\Omega_{tr}^2 = \frac{1}{2}(I_{mr}+\tau^2 I_{tr})\Omega_{mr}^2$$

The energy conservation equation for the system Engine-Rotors is given by:

$$\frac{dT_{rotors}}{dt} = P_e - P_{rotors}$$

Thus

$$(I_{mr}+\tau^2 I_{tr})\Omega_{mr}\dot{\Omega}_{mr} = P_e - P_{rotors}$$

Where P_e is the power provided by the engine and P_{rotors} is the power absorbed by the rotors which can be written as:

$$P_{rotors} = Q_{mr}\cdot\Omega_{mr} + Q_{tr}\cdot\Omega_{tr} = (Q_{mr}+\tau Q_{tr})\Omega_{mr}$$

When the Engine is on, a control system keeps rotational speeds constant varying the engine power. In the Engine off case, as in autorotation, the term P_e is zero and the equation becomes:

$$(I_{mr}+\tau^2 I_{tr})\Omega_{mr}\dot{\Omega}_{mr} = -(Q_{mr}+\tau Q_{tr})\Omega_{mr}$$

Which gives:

(14) $$\dot{\Omega}_{mr} = -\frac{(Q_{mr}+\tau Q_{tr})}{I_{mr}+\tau^2 I_{tr}} \cong -\frac{Q_{mr}}{I_{mr}}$$

Where tail rotor influence has been neglected**.**

All the previous equations are nonlinear with respect to the state vector, and they are all coupled.

2.1.3. Attitude Kinematics

The attitude of the rotorcraft is expressed by means of Euler Angles $[\Phi\ \Theta\ \Psi]'$ which varies in time as a function of $\boldsymbol{\omega_b}$ as follows:

(15) $$\begin{bmatrix}\dot{\phi}\\ \dot{\Theta}\\ \dot{\Psi}\end{bmatrix} = \begin{bmatrix}1 & \sin\phi\tan\Theta & \cos\phi\tan\Theta\\ 0 & \cos\phi & -\sin\phi\\ 0 & \frac{\sin\phi}{\cos\Theta} & \frac{\cos\phi}{\cos\Theta}\end{bmatrix}\boldsymbol{\omega_b}$$

The velocities in Earth inertial axes are written as function of Euler angles and velocities in body frame:

(16) $$\begin{bmatrix}\dot{x}\\ \dot{y}\\ \dot{z}\end{bmatrix} = \boldsymbol{\Pi_{Eb}}\begin{bmatrix}u\\ v\\ w\end{bmatrix}$$

(17) $$\boldsymbol{\Pi_{Eb}} = \begin{bmatrix}c\Theta c\Psi & s\phi s\Theta c\Psi - c\phi s\Psi & c\phi s\Theta c\Psi + s\phi s\Psi\\ c\Theta s\Psi & s\phi s\Theta s\Psi + c\phi c\Psi & c\phi s\Theta s\Psi - s\phi s\Psi\\ -s\Theta & s\Phi c\Theta & c\phi c\Theta\end{bmatrix}$$

2.1.4. Main rotor

The hinge less Rotor is modelled as a teetering one where an equivalent rotor flapping stiffness K_β is introduced as a correction of the ideal teetering model. Flapping dynamics is approximated using a tip-path plane representation. The following assumptions are introduced:

1. Rotor blade is rigid in bending and torsion;
2. Linear blade twist;
3. Flapping and inflow angles are assumed small, the analysis is based on a simple strip theory;
4. Only effects due to angular acceleration $\dot{p}$ and $\dot{q}$, angular velocity p, q and the normal acceleration of the aircraft motion are considered to calculate blade flapping;
5. Compressibility and stall effects are not considered;
6. Reversed flow region is not considered;
7. The inflow is assumed to be uniform;
8. The tip loss factor is assumed to be 1;

9. Blade flapping is approximated by the first harmonic terms with time-varying coefficients as in equation (12).

According to blade flapping approximation in equation (12), a_0 is treated as a pre-set constant and coefficients $a_1(t)$ and $b_1(t)$ can be evaluated considering $\dot{a}_0 = \ddot{a}_0 = 0$ in equation (11).

The analytical evaluation of main rotor forces and moments is done using the blade-element theory. The total force on a blade having a ψ azimuth is obtained integrating the force on the blade element over the rotor radius. Then the integration with respect to the azimuth $\psi = [0; 2\pi]$ gives the mean force of the blade over a complete rotation around the shaft. Equations are first obtained in the Wind-Hub coordinate system and then transformed into Body system. Complete derivation of Main rotor forces is given in [6] where the only difference with respect to our assumptions is that in [6] a static-uniform inflow is used, while we adopted a dynamic-uniform inflow.

2.1.5. Clockwise correction factors

The equations derived in [4] [6] [7] are valid for a counter-clock-wise rotor. When the rotation is clock-wise a correction factor needs to be add Introducing a parameter χ which value is equal to 1 when rotor is counter-clockwise; -1 otherwise. Resulting equations are given as follows:

$$\begin{aligned} \boldsymbol{V}_{cl} &= \Pi_1 \boldsymbol{V}_{ccl} \\ \boldsymbol{\omega}_{cl} &= \Pi_2 \boldsymbol{\omega}_{ccl} \\ \boldsymbol{F}_{cl} &= \Pi_1 \boldsymbol{F}_{ccl} \\ \boldsymbol{M}_{cl} &= \Pi_2 \boldsymbol{M}_{ccl} \\ [\theta_0\ A_{1s}\ B_{1s}]'_{cl} &= \Pi_1 [\theta_0\ A_{1s}\ B_{1s}]'_{ccl} \end{aligned} \tag{18}$$

provided $\Pi_1 = \begin{bmatrix} 1 & 0 & 0 \\ 0 & \chi & 0 \\ 0 & 0 & 1 \end{bmatrix}$, $\Pi_2 = \begin{bmatrix} \chi & 0 & 0 \\ 0 & 1 & 0 \\ 0 & 0 & \chi \end{bmatrix}$

2.1.6. Tail rotor

Tail rotor is modelled as in [7], where flapping dynamics is ignored and a steady state solution for flapping angles, Forces and Moments is considered. The inflow ratio is here static and uniform and it is obtained as a steady state of a Pitt-Peters model:

$$\lambda_{tr} = -\frac{v_{tr}}{\Omega_{tr} R_{tr}} - \frac{C_{t,tr}}{2\sqrt{\mu_{tr}^2 + \lambda_{tr}^2}} \tag{19}$$

This equation needs to be solved with a Newton-Ralphson method for every time step.

2.1.7. Fuselage

The Fuselage Forces and Moments are evaluated as a function of the angle of attack and the sideslip angle. Aerodynamic coefficients are obtained with estimated look-up tables. Main equations are:

$$\begin{aligned} \boldsymbol{V}_{\boldsymbol{fus}} &= \boldsymbol{V}_{\boldsymbol{b}} + \boldsymbol{\omega}_{\boldsymbol{b}} \times \boldsymbol{r}_{\boldsymbol{fus}} \\ \alpha_{fus} &= \operatorname{atan} \frac{w_{fus}}{u_{fus}} \\ \beta_{fus} &= \operatorname{asin} \frac{v_{fus}}{|V_{fus}|} \\ D &= \frac{1}{2} \rho |V_{fus}|^2 S_{ref} C_D(\alpha, \beta) \\ Y &= \frac{1}{2} \rho |V_{fus}|^2 S_{ref} C_Y(\alpha, \beta) \\ L &= \frac{1}{2} \rho |V_{fus}|^2 S_{ref} C_L(\alpha, \beta) \end{aligned}$$

(20)

$$\boldsymbol{F}_{\boldsymbol{fus}}^{\boldsymbol{a}} = \begin{bmatrix} -\cos\alpha_{fus}\cos\beta_{fus} & -\sin\alpha_{fus}\sin\beta_{fus} & \sin\alpha_{fus} \\ -\sin\beta_{fus} & \cos\beta_{fus} & 0 \\ -\sin\alpha_{fus}\cos\beta_{fus} & -\sin\alpha_{fus}\sin\beta_{fus} & \cos\alpha_{fus} \end{bmatrix} \begin{pmatrix} D \\ Y \\ L \end{pmatrix}$$

$$\boldsymbol{M}_{\boldsymbol{fus}}^{\boldsymbol{a}} = \boldsymbol{r}_{\boldsymbol{fus}} \times \boldsymbol{F}_{\boldsymbol{fus}}^{\boldsymbol{a}}$$

Where $\boldsymbol{r}_{\boldsymbol{fus}}$ is the position of the fuselage pressure center with respect to gravity center of the rotorcraft.

2.1.8. Gravitational force

Helicopter weight force in body axes is written as:

$$\boldsymbol{W}_{\boldsymbol{b}} = Mtot \cdot g \cdot \begin{bmatrix} \sin\Theta \\ \sin\phi\cos\Theta \\ \cos\phi\cos\Theta \end{bmatrix} \tag{21}$$

2.2. Design of a suitable autorotation maneuver

Helicopter autorotation is a safe landing maneuver which needs to be performed in the case of total power loss. It can be divided in three main phases: entry, steady descent, and flare.

When the Engine is Off the rotor aerodynamic torque is no more equilibrated by the engine and the rotor speed starts decreasing. This makes the thrust decreasing, and the helicopter starts a descent. The impinging flow can reduce aerodynamic torque keeping a certain level of rotor speed. In this case the rotor is in wind-mill-state and provides a residual thrust which contrast the gravitational force reducing the sink rate. A steady descent is then possible

calibrating collective pitch such that constant rpms are kept. The value of this rotational speed is a function of the sink rate and needs to be optimized to keep a sufficient level of rotational energy to perform the final flare. This last phase is done to reduce sink rate and advancing velocity to minimum values at touch down, exploiting all the residual energy to produce a braking force. Decreasing rotor speed under minimum acceptable level during the steady descent prevents the rotor from generating the thrust necessary for a safe landing. Acceptable values for touch down velocities and final attitude are set to:

$$\begin{cases} u_{E_{max,TD}} = 0.5\ m/s \\ v_{E_{max,TD}} = 0.5\ m/s \\ w_{E_{max,TD}} = 0.25\ m/s \\ -10° < \Phi_{\mathrm{TD}} < 10° \\ -10° < \Theta_{\mathrm{TD}} < 10° \end{cases} \tag{22}$$

In this work no constraints are considered on the helicopter final position. Then an infinite extended landing field is assumed, and a pure longitudinal and ideally rectilinear maneuver is modelled.

2.2.1. Steady descent

All the possible steady descent conditions have been evaluated considering the whole mathematical model and calculating equilibrium conditions for imposed advancing velocities u_e and sink rates w_e:

Imposed conditions:

$$\begin{cases} \boldsymbol{V_E} = [u_E\ 0\ w_E]' \rightarrow \boldsymbol{V_b} = \boldsymbol{\Pi_{bE}}(\Phi, \Theta) \cdot \boldsymbol{V_E} \\ \boldsymbol{\omega_b} = [0\ 0\ 0]' \\ \dot{\boldsymbol{a}} = [0\ 0\ 0]' \end{cases} \tag{23}$$

Resulting problem:

$$\begin{cases} \dot{\boldsymbol{V}}_{\boldsymbol{b}} = -\boldsymbol{\omega_b} \times \boldsymbol{V_b} + \frac{\boldsymbol{F_b}}{M_{tot}} = \boldsymbol{0} \\ \dot{\boldsymbol{\omega}}_{\boldsymbol{b}} = \boldsymbol{I}^{-1}[-\boldsymbol{\omega_b} \times (\boldsymbol{I}\boldsymbol{\omega_b}) + \boldsymbol{M_b}] = \boldsymbol{0} \\ \ddot{\boldsymbol{a}} = -\tilde{\boldsymbol{D}}\dot{\boldsymbol{a}} - \tilde{\boldsymbol{K}}\boldsymbol{a} + \tilde{\boldsymbol{f}} = \boldsymbol{0} \\ \dot{\lambda}_i = \frac{3\pi}{4}\left\{\frac{C_t}{2} - \lambda_i\sqrt{\mu^2 + \lambda^2}\right\} = 0 \\ \dot{\Omega} = -\frac{Q_{mr}}{I_{mr}} = 0 \end{cases} \rightarrow \tag{24}$$

$$\begin{cases} \boldsymbol{F_b}(\boldsymbol{V_E}, \boldsymbol{a}, \boldsymbol{u}, \Phi, \Theta, \lambda, \Omega) = \boldsymbol{0} \\ \boldsymbol{M_b}(\boldsymbol{V_E}, \boldsymbol{a}, \boldsymbol{u}, \Phi, \Theta, \lambda, \Omega) = \boldsymbol{0} \\ \boldsymbol{f_a}(\boldsymbol{V_E}, \boldsymbol{a}, \boldsymbol{u}, \Phi, \Theta, \lambda, \Omega) = \boldsymbol{0} \\ f_\lambda(\boldsymbol{V_E}, \boldsymbol{a}, \boldsymbol{u}, \Phi, \Theta, \lambda, \Omega) = 0 \\ Q_{mr}(\boldsymbol{V_E}, \boldsymbol{a}, \boldsymbol{u}, \Phi, \Theta, \lambda, \Omega) = 0 \end{cases}$$

The problem is a nonlinear system of 11 equations in 11 unknowns (10x10 considering $a_0 = cost$) and it has been solved using a Newton method based on the numerical evaluation of the Jacobian matrix of the system.

In Figure 1 is shown the steady descent rotational speed Ω as a function of the sink rate w_E and advanced velocity u_E while the corresponding collective pitch is visible in Figure 2. Fixing an advancing velocity u_E, the sink rate is reduced when reduced rotor speeds are considered, while the collective pitch increases. Then, when the collective is kept higher the rotor delivers a higher thrust reducing sink rate, but consuming energy stored (rotor rpms). A compromise needs to be found between w_E and Ω, where the first should be minimized and the second should be maximized.

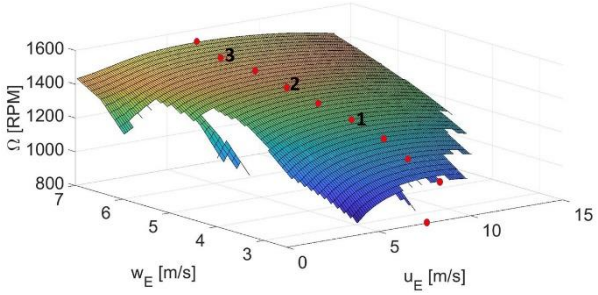

Figure 1: Rotor speed in autorotation steady descent

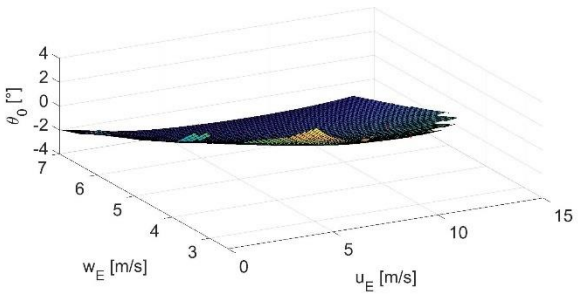

Figure 2: Collective pitch for autorotation steady descent

Again, in Figure 1 can be seen that moving on $w_E = cost$ curves, rotor speed has a maximum for advancing velocities around 7-9 m/s. In fact, lower levels of V reduces dynamic pressure, higher collective is needed to obtain the necessary thrust, and then lower rotor speed results. On the other hand, higher velocities need a pitched attitude then a reduced inflow, and again minor rotor speed.

Red points in Figure 1 are obtained choosing the higher Ω for fixed values of w_E. The choice of the best steady state condition is made simulating the flare starting from points 1,2, 3 in Figure 1 and evaluating which one gives the best trajectory.

2.2.2. Flare

The last phase of the autorotation must bring the helicopter to minimum velocity at touch down. Collective pitch must be increased producing the thrust needed to decelerate. To investigate which is the best command law, an open loop command has been implemented to simulate how the system responds imposing as initial condition, one of the steady descent conditions evaluated before (1,2, 3). The open loop command has an exponential form such that collective is continuous with the initial value of the steady descent and ideally increases to its maximum value.

$$\theta_0(t) = \theta_{0,sd} + (\theta_{0,max} - \theta_{0,sd})(1 - e^{-\frac{t}{\tau}}) \quad (25)$$

In Figure 3 it is shown the results of this simulation for different values of τ when steady descent condition 2 is adopted as initial condition. Here a first value for the flare starting altitude is set to $h_{flare} = 10m$. How expected the rate of descent starts to decrease and after a minimum, it increases again. This is because after that minimum, rotor speed is no more sufficient to contrast the weight force and the rotorcraft falls accelerating. It is possible to choose τ such that the minimum velocity corresponds to zero. A new value of h_{flare} can be then evaluated to have the minimum velocity at touch down (Figure 4).

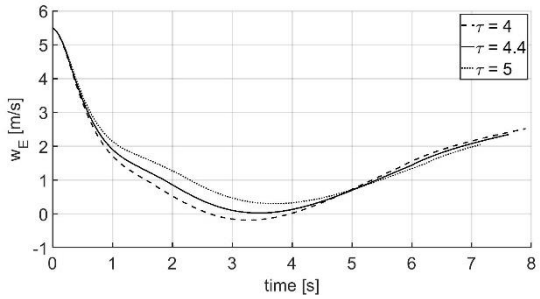

Figure 3: Vertical velocity during flare in open loop

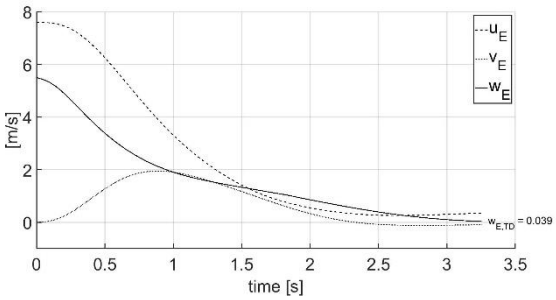

Figure 4: Helicopter velocity during flare in open loop, with calculated initial altitude ($\tau = 4.4$)

Similar simulations have been performed for the three different steady descent points. Results are shown in Table 1. Here in all the cases the touch down velocity is under the imposed limit of 0.25 m/s. Looking at the initial altitude and the time for the flare it can be noticed that, as expected, a higher rotor energy permit a less impulsive maneuver while a reduced time and altitude are needed in the case of lower rotor angular rates. The drawback is that choosing Ω_{sd} too much high can give problems because the control system usually recognizes the engine failure with a time delay. Therefore if the rotor rate falls under the steady descent nominal value before the control system starts the autorotation, control system could have problem to restore higher rotation rates and a lower and more problematic entry in the steady descent could results.

Thus condition #2 of the table is chosen as the best.

#	Ω_{sd} $[rpm]$	$u_{E,sd}$ $[m/s]$	$w_{E,sd}$ $[m/s]$	$\theta_{0,sd}$ $[°]$	τ	h_{flare} $[m]$	$w_{E,TD}$ $[m/s]$	t_{flare} $[s]$
1	1234	8.5	4.5	-0.74	4.55	2.8	0.086	2.44
2	1363	7.5	5.5	-1.89	4.4	5.3	0.039	3.25
3	1475	6.5	6.5	-2.93	4.1	7.9	0.042	3.47

Table 1: Open loop flare results for three initial steady descent conditions.

2.3. Control system for autorotation

A different control strategy has been designed for the different phases of autorotation. A first logic permits to recognize the phases of autorotation:

- When Ω decrease under a minimum value $\Omega_{decision}$ the system switches from the Engine ON control system to the autorotation control.
- When the altitude h is equal to h_{flare} a second logic is activated to perform the flare.

2.3.1. Stabilizer logic for pitch and roll

A basic stabilizer logic is used in normal flight conditions. The scheme is reported in Figure 5. In both cases, an inner loop controls pitch/roll rates while, with an outer loop, a desired pitch/roll angle is compared with the actual attitude and the error generated becomes a reference for the inner loop.

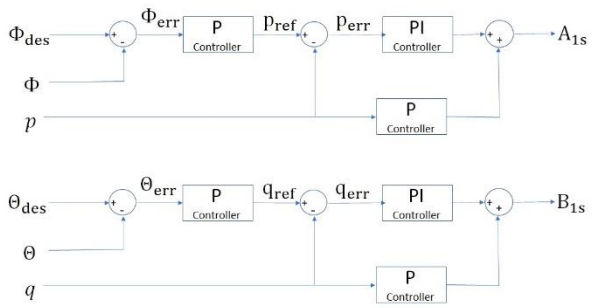

Figure 5: Roll and Pitch stabilizer

2.3.2. Heading Hold Logic

The Heading Hold logic is shown in Figure 6. The desired yaw rate is compared with the actual yaw rate and the error is integrated to obtain an estimated yaw error. The latter is used to elaborate a desired yaw rate that again, compared with the actual yaw rate generates the error used to elaborate θ_{tr}. A fixed θ_{tr0} is added to consider the tail rotor thrust needed to balance main rotor torque at hovering. Another contribution for θ_{tr} is finally proportional to θ_0 and takes into account how tail rotor thrust needs to modulate as a function of main rotor torque, and thus as a function of collective command.

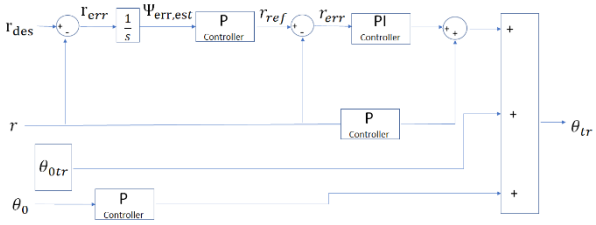

Figure 6: Heading Hold

2.3.3. Steady descent control logic

For the steady descent, the strategy is to bring the system to the chosen condition evaluated before, namely Ω_{sd},$u_{E_{sd}}$,$w_{E_{sd}}$. This is done implementing a control on Ω and u_e as shown in Figure 7. Here, in the first phase, collective pitch is set to the nominal value $\theta_{0,sd}$.When rotor speed decreases under the nominal value, a PI feedback control on Ω elaborates the collective pitch θ_0 keeping $\Omega = \Omega_{sd}$. At the same time, the error between the desired velocity and the actual one $u_{E_{sd}} - u_E$ generates the reference Pitch angle given to the Pitch stabilizer to elaborate the longitudinal control B_{1s}. Similar control is done for A_{1s} where a reference zero lateral velocity $v_E$is used to elaborate a reference roll angle for the roll stabilizer. Finally, the tail is controlled by the heading hold, where θ_{tr0} is set to zero considering that thanks to the free-wheel mechanism the rotor torque is no more discharged to the fuselage in autorotation.

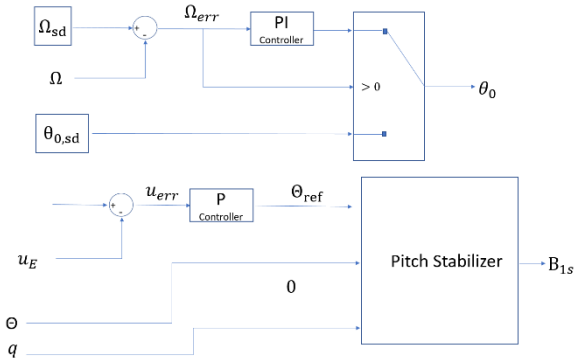

Figure 7: Steady descent control

2.3.4. Flare control logic

The control logic is shown in Figure 8, where an altitude hold with a variable reference is implemented. Considering again the best open loop flare calculated in section 2.2.2 it is possible to notice from Figure 9 that the velocity is almost linear with the altitude and therefore altitude profile can be approximated with a pure exponential function. Then our reference trajectory can be expressed as:

(26) $$h_{ref}(t) = h_{flare}\, e^{-\frac{t}{\tau_{cl}}}$$

$$w_{E_{ref}}(t) = -\frac{dh_{ref}(t)}{dt} = \frac{h_{flare}}{\tau}\, e^{-\frac{t}{\tau_{cl}}} = \frac{h_{ref}(t)}{\tau_{cl}}$$

The τ_{cl} coefficient can be estimated considering Figure 9, where altitude and vertical velocity variation during the open loop flare are compared. Approximating the real plot with a regression line it is possible to evaluate τ_{cl} as the slope of the line according to eq.(26).

In this way it is possible to elaborate a closed loop control system for the flare, where the reference altitude is calculated, for every time step, multiplying $\boldsymbol{\tau_{cl}}$ and the actual value of the rate of descent.

Finally, the advancing velocity is reduced giving to the pitch stabilizer a reference pitch angle evaluated from the actual velocity.

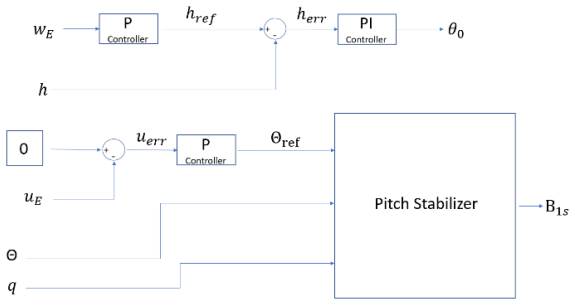

Figure 8: Flare control system

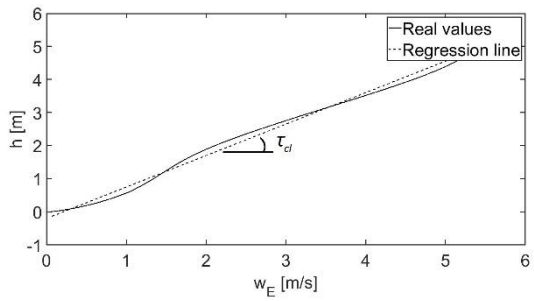

Figure 9: Altitude vs sink rate during open loop flare

3. SIMULATIONS

3.1.1. Simulations parameters

The complete autorotation landing has been simulated implementing the described model on Simulink. Main Helicopter parameters for the Goblin Saab 700 Helicopter used here, can be found in **Error! Reference source not found.**,**Error! Reference source not found.** and **Error! Reference source not found.**. For all the simulations the following assumptions are considered:

- Infinite extended landing field and no constraints on final position
- Engine failure happens after $\mathbf{5}\boldsymbol{s}$ of stable level flight
- The control system recognizes the engine failure and starts the autorotation when $\boldsymbol{\Omega} < \boldsymbol{\Omega_{decision}}$ which is set to 95% of the value for normal flight
- Constraints for a safe autorotation landing are reported in equation (22).
- During autorotation, the control system brings the helicopter to the nominal steady descent condition #2, and then perform the flare as described in previous sections.

3.2. Autorotation for nominal initial conditions

Nominal initial conditions are $\boldsymbol{h_0} = \mathbf{200}\boldsymbol{m}$ and $\boldsymbol{V_E}\mathbf{0} = [\mathbf{7.5\ 0\ 0}]'\ \boldsymbol{m/s}$. Simulation results are reported in Figure 10. After the engine failure at 5s, the vertical velocity starts to increase while the rotor speed decreases. An instant yaw displacement appears because the tail rotor continues for few instants to deliver a thrust to counteract main rotor torque which is no more discharged on the fuselage thanks to the free wheel mechanism. The rotorcraft is then brought to nominal steady descent conditions ($\boldsymbol{\Omega} = \mathbf{1363}\ \boldsymbol{rpm}\ ; \boldsymbol{w_E} = \mathbf{5.5}\ \boldsymbol{m/s}$) and when $\boldsymbol{h_{flare}}$ is reached, the collective starts to increase while the pitch command decreases, reducing sink rate and advancing velocity.

3.3. Behaviour for different velocities

Three simulations at different initial velocity have been performed to evaluate how the helicopter react to the control system. Results are shown in Figure 11. In all the cases the helicopter performs the steady descent and the flare in a good way, reaching acceptable touch-down velocities and attitude.

3.4. Behaviour for different altitudes

The influence of the initial altitude on the success of the designed autorotation maneuver is investigate simulating three different initial altitudes and the nominal initial velocity. Results are plot in Figure 12.What happens is that, for $\boldsymbol{h_0} = \mathbf{200}\boldsymbol{m}$, steady descent and flare are regularly performed, while reducing the initial altitude the time for steady descent reduces since for $\boldsymbol{h_0} = \mathbf{10}\boldsymbol{m}$ the altitude is already adequate to just perform the flare. All the simulation gives acceptable autorotation landing.

4. CONCLUSIONS

This paper presented preliminary results of an automatic autorotation maneuver for a small-scale unmanned helicopter, with a particular on the analysis of the steady descent conditions. Helicopter dynamics was modelled by means of a 10 DOF nonlinear system, and an algebraic system has been iteratively solved for deriving the trim variables. What results is that, high values of rotor speed, require low values of collective pitch, driving to high rate of descent as well as high inflow, necessary for the wind-mill state. Thus, during the steady descent a trade-off between the sink rate (which should be limited) and the rotor speed is a mandatory task.

Steady descent conditions affect the flare manoeuvre: high values of rotor rate allows for a less aggressive pull-up maneuver. On the other hand, nominal value of Ω_{sd} should not be chosen too much close to the normal flight value: control system starts autorotation control with a time delay with respect to engine fail, therefore if the rotor rate falls under the nominal value before the autorotation control is active, a more complicated and problematic maneuver can results.

On the basis of obtained results, an off-line autorotation pattern has been designed and a closed loop control system has been developed to follow it. The simulations for nominal initial altitudes and velocity shown that the control system is capable to bring the helicopter to steady descent and then to perform the flare reducing touch down velocities under acceptable limits. Robustness with respects different initial condition has been also

demonstrated. For variable initial altitude it results that lowering the altitude autorotation is successful even if, as expected, the steady descent time is reduced.

Parameters		Value	Unit
Total mass	M_{tot}	4.8	kg
Inertia moments	I_{xx}	0.0465	$kg \cdot m^2$
	I_{yy}	0.2971	$kg \cdot m^2$
	I_{zz}	0.2567	$kg \cdot m^2$
Inertia products	I_{xy}	0.0079	$kg \cdot m^2$
	I_{xz}	0.0033	$kg \cdot m^2$
	I_{yz}	0.0006	$kg \cdot m^2$

Table 2: Mass and Inertia parameters for Goblin Saab 700 Helicopter

Parameters		Value	Unit
Tail Rotor speed in normal flight	$\Omega_{tr,100\%}$	9976	rpm
Tail Rotor Radius	R_{tr}	0.115	m
Number of blades	$N_{b_{tr}}$	2	$--$
Tail Rotor solidity	σ_{tr}	0.1716	$--$
Tail rotor position in body axes	$r_{tr} = \begin{bmatrix} x_h \\ y_h \\ z_h \end{bmatrix}$	$\begin{bmatrix} -1.045 \\ 0.052 \\ -0.031 \end{bmatrix}$	m

Table 3: Tail rotor parameters for Goblin Saab 700 Helicopter

Parameters		Value	Unit
Rotation direction	χ	$-1\ Clockwise$	$--$
Rotor speed in normal flight	$\Omega_{100\%}$	1995	rpm
Radius	R	0.79	m
Rotational Inertia	I_{mr}	0.0689	$kg \cdot m^2$
Number of blades	N_b	2	$--$
Virtual Hinge Offset ratio	ε	0.0314	$--$
Airfoil lift slope	Cl_α	2π	$1/rad$
Airfoil chord	c	0.06	m
Blade mass	m_b	0.2057	kg
Blade inertia about flapping hinge	I_b	0.0344	$kg \cdot m^2$
Flapping stiffness	K_β	162.69	$N \cdot m/rad$
Pitch-Flap coupling	K_1	0	$--$
Blade twist	θ_t	0	rad/m
Rotor solidity	σ	0.0479	$--$
Rotor shaft tilt angle	i_s	0.0524	rad
Precone	a_0	0	rad
Hub position in body axes	$r_h = \begin{bmatrix} x_h \\ y_h \\ z_h \end{bmatrix}$	$\begin{bmatrix} 0.0095 \\ 0 \\ -0.1810 \end{bmatrix}$	m

Table 4: Main rotor parameters for Goblin Saab 700 Helicopter

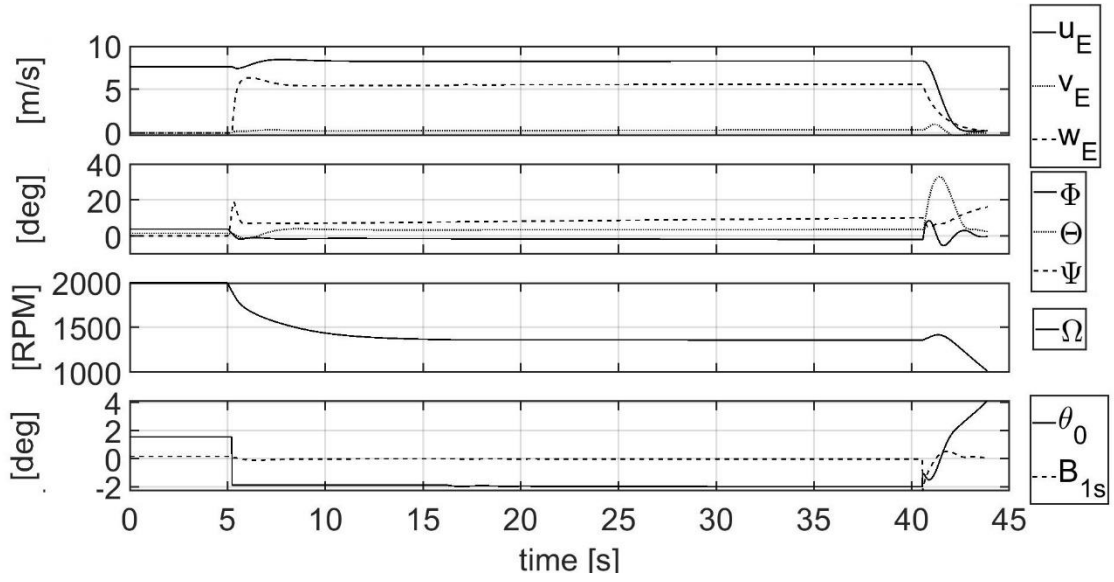

Figure 10: Simulation results for $h_0 = 200m$ and $u_{E0} = 7.5m/s$

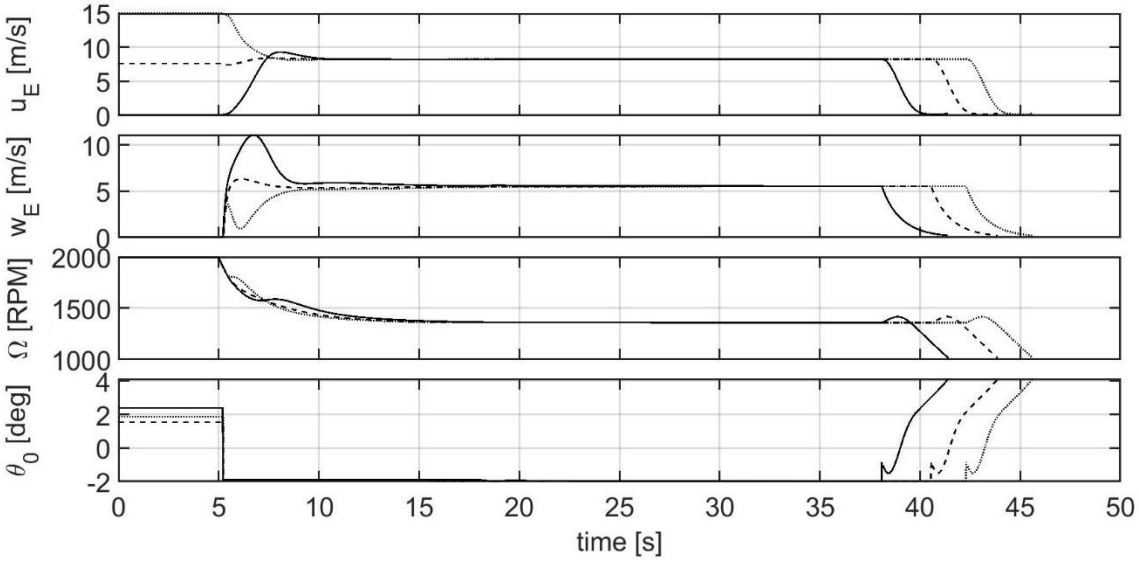

Figure 11: Simulation results for different initial velocities (—$hovering$; $--7.5\ \frac{m}{s}$; $\cdots 15\frac{m}{s}$) and $h_0 = 200m$

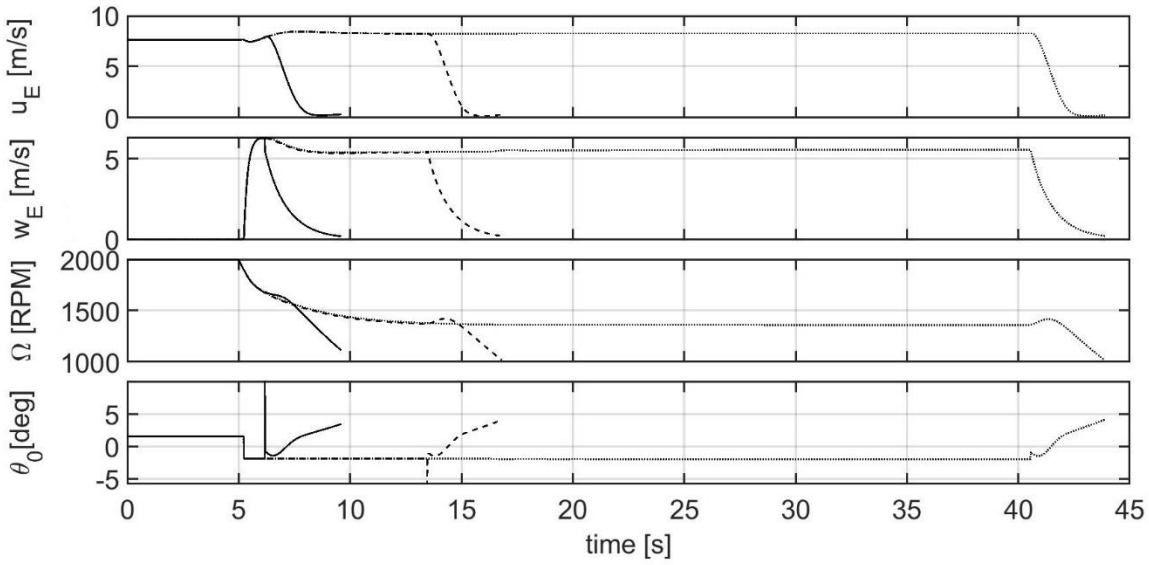

Figure 12: Simulation results for different initial altitudes $(—10m;\ --50m;\ \cdots 200m)$ *and* $u_{E0} = 7.5\ m/s$

REFERENCES

[1] W. Johnson, «Helicopter optimal descent and landing after power loss,» May 1977.

[2] P. Bibik e J. Narkiewicz, «Helicopter Optimal Control After Power Failure Using Comprehensive Dynamic Model,» *Journal Of Guidance, Control, ans Dynamics,* vol. 35, n. 4, pp. 1354-1362, July–August 2012.

[3] S. Taamallaha, X. Bomboisb e P. M. Van den Hofc, «Trajectory planning and trajectory tracking for a small-scale helicopter in autorotation,» *Control Engineering Practice,* n. 58, p. 88–106, 2017.

[4] R. T. N. Chen, «Effects of primary rotor parameters on Flapping Dynamics,» *NASA Technical Paper 1431,* January 1980.

[5] D. Peters e N. HaQuang, «Dynamic Inflow for practical applications,» *Journal of American Helicopter Society TN,* October 1988.

[6] R. T. N. Chen, «A simplified rotor system mathematical model for piloted flight dynamics simulation,» Ames Reaserach Center, NASA, Moffett Field, California, May 1979.

[7] P. D. Talbot, B. E. Tinling, W. A. Decker e R. T. N. Chen, «A mathematical model for a single main rotor helicopter for piloted simulation,» Ames Reasearch Center, Moffett, Field, California, September 1982.